16. MAGNETIC PROPERTIES AND ALTERATION IN BASALT, HOLE 504B, DEEP SEA DRILLING PROJECT LEG 83[1]

H. Kinoshita, Department of Earth Science, Chiba University
and
Toshio Furuta and Hodaka Kawahata, Ocean Research Institute, University of Tokyo[2]

ABSTRACT

We report measurements of magnetic intensity, inclination, initial susceptibility, Koenigsberger's ratio, saturation magnetization, and Curie temperatures of 68 basalt samples from the Leg 83 section of Hole 504B. As in the upper part of the hole, reversely magnetized units predominate. Intensities of natural remanent magnetization vary widely, but the range of variation is an order of magnitude less than in the upper part of the hole. This and the other properties measured indicate that the magnetic characteristics of basalts from Hole 504B have been strongly affected by hydrothermal alteration, particularly in the deeper, Leg 83 section. The alteration states of the magnetic samples were studies using X-ray diffraction, electron microprobe, X-ray fluorescence, and ion coupled plasma. Our results suggest three alteration zones in Hole 504B: a low-temperature zone (274.5–890 m) and two high-temperature zones (890–1050 m and 1050–1350 m), differing in the number of veins observed in the samples and presumably differing in the volumes of hydrothermal fluids which reacted with the basalts.

INTRODUCTION

Hole 504B is located on the southern flank of the Costa Rica Rift. The age of the basement at Site 504 is estimated to be 5.9 m.y., based on the magnetic anomaly pattern. (This area displays reversed remanent magnetization.) Hole 504B was started by Leg 69 shipboard party and reached 1350 m beneath the seafloor (BSF) during drilling on Legs 69, 70, and 83. The basement section consists of alternating sequences of pillow and massive basalts; only massive formations and sheeted dikes were cored below 1055 m BSF. This report presents a series of data on rock magnetic parameters and related mineralogical alteration of basalt samples from the Leg 83 section of Hole 504B (836–1350 m BSF). Furuta (1983) and Furuta and Levi (1983) presented similar data on samples from Legs 69 and 70 basement sections of Hole 504B. In the first section, paleomagnetic, rock magnetic, and magneto-mineralogical analyses are described. In the second section, data concerning the hydrothermal alteration found in the paleomagnetic rock samples are briefly presented in light of the paleomagnetic data.

MAGNETIC PROPERTIES OF BASALT SAMPLES

Measurements of magnetic properties were carried out on 68 homogeneous basalt samples recovered during Leg 83. Magnetic susceptibility, intensity, and inclination had been measured on board *Glomar Challenger* on the same samples (Hole 504B summary chapter, this volume); we repeated the measurement of these parameters. Methods used for our shore-based studies were those described by Furuta (1983) and Furuta and Levi (1983). The results of our measurements of natural remanent magnetization (NRM), initial susceptibility, and thermomagnetic properties are listed in Table 1.

Intensity of Natural Remanent Magnetization (J_n)

The intensity of NRM (J_n) is widely scattered, ranging from 0.09 to 36 x 10^{-4} gauss. A wide variation of NRM was also observed in the upper part of Hole 504B (Furuta and Levi, 1983). However, the range of J_n in the lower part of the hole is an order of magnitude smaller than that in the upper part. J_n versus depth is shown in Figure 1. J_n depends little on the depth but rather seems to depend on grain-size distribution of ferromagnetic minerals as well as on the degree of hydrothermal alteration of individual rock samples. Several features are conspicuous: very low J_n in pillow units, and relatively high J_n in massive flows near the bottom of the hole.

Pillow lavas usually show high J_n because fine magnetic minerals are present. However, the lowest J_n of this hole (less than 10^{-4} gauss) is found in a pillow lava sequence. Relatively high J_n is found in a massive flow near the bottom of the hole that is composed of coarse-grained doleritic or micro-gabbroic rocks. These exceptions to the general trend seem to depend upon hydrothermal alteration of individual rock samples.

Inclination (I_s)

Magnetic remanence vectors of all the available minicores were remeasured by a spinner magnetometer in the shore laboratory. The stable inclinations plotted in Figure 2 are used to define 16 magnetic units, which include various lithologic units. Table 2 shows the average magnetic properties of each unit. Reversely magnetized units predominate through the hole, which is consistent with the polarity of the upper part of the hole (Furuta and Levi, 1983). There are a few polarity changes, of which one steep inclination zone was observed. A simi-

[1] Anderson, R. N., Honnorez, J., Becker, K., et al., *Init. Repts. DSDP*, 83: Washington (U.S. Govt. Printing Office).

[2] Addresses: (Kinoshita) Department of Earth Science, Chiba University, 1-33 Yayoi-cho, Chiba 260, Japan; (Furuta, Kawahata) Ocean Research Institute, University of Tokyo, Nakano, Toyko 165, Japan.

Table 1. Paleomagnetic results, Hole 504B, Leg 83.

Core-Section (interval in cm)	Sub-bottom depth (m)	J_n ($\times 10^{-4}$ gauss)	I_s (°)	k ($\times 10^{-4}$ gauss/Oe)	Q_n	MDF (Oe)	J_s (emu/g)	Magnetic unit
71-1, 127-129	837.28	33.6	80.6	34.4	2.7	120	1.14	0
72-2, 105-107	846.06	14.3	−14.0	20.8	1.9	145	1.41	
73-1, 87-89	853.06	19.1	−7.4	18.6	2.9	240	1.50	
73-2, 93-95	854.94	2.6	−8.0	26.3	0.3	110	1.64	
74-1, 94-96	862.45	13.5	−10.7	28.8	1.3	155	1.78	
75-1, 9-11	870.60	12.7	−32.6	24.4	1.4	145	1.64	
76-1, 24-26	879.75	6.6	−18.1	20.0	0.9	210	0.71	1a
77-1, 23-25	888.74	6.2	−11.4	24.9	0.7	130	1.89	
77-3, 14-16	891.65	1.8	(3.5)	27.5	0.2	130	1.56	
78-1, 42-44	897.93	7.5	−16.0	23.0	0.9	150	2.58	
79-1, 96-98	905.47	8.7	−10.0	11.0	2.2	260	0.68	
79-3, 110-113	908.62	4.5	−21.8	6.4	1.9	280	0.40	
80-1, 122-124	911.23	0.14	−6.9	1.2	0.3	400	0.06	
81-1, 114-116	920.65	0.33	−17.0	1.9	0.5	260	0.12	
82-1, 21-23	928.72	0.17	−12.0	0.9	0.5	330	0.12	1b
82-2, 111-113	931.12	0.75	−20.0	5.3	0.4	170	0.39	
83-1, 33-35	937.84	0.17	−6.3	0.9	0.5	300	0.08	
84-1, 134-136	947.80	0.29	−35.0	1.5	0.5	310	0.11	
85-2, 75-77	957.76	9.3	0	9.4	2.8	250	0.78	2a
87-1, 85-87	967.86	2.5	−52.3	1.5	4.6	380	0.12	2b
87-2, 8-10	968.69	2.3	16.9	1.3	4.9	460	0.10	2c
88-1, 15-17	976.66	0.09	−21.0	0.4	0.6	350	0.09	3a
89-1, 100-103	986.52	0.74	−42.8	0.9	2.3	280	0.11	
90-2, 101-104	997.03	0.09	−75.0	11.0	2.3	230	0.19	3b
90-4, 143-146	1000.45	0.38	−69.0	1.1	0.96	410	0.11	
92-3, 67-69	1016.18	2.5	−6.8	2.2	3.2	270	0.11	
93-2, 81-83	1023.82	0.6	−11.0	2.4	0.7	380	0.19	4
93-3, 66-68	1025.17	0.31	−6.2	1.4	0.6	340	0.09	
94-1, 107-109	1031.58	7.2	7.2	10.9	1.8	250	1.14	5
94-3, 82-84	1034.33	7.7	12.7	13.7	1.6	250	1.17	
95-1, 100-102	1040.51	10.3	−6.4	6.4	4.5	330	0.55	6a
98-1, 78-80	1062.79	1.54	−40.0	1.4	3.1	250	0.09	
99-1, 69-71	1072.20	34.5	−24.1	9.7	9.9	230	1.00	6b
100-1, 21-23	1080.72	6.7	−23.6	1.9	9.7	420	0.15	
100-3, 20-22	1083.72	4.6	7.2	2.4	6.7	240	0.12	7
101-1, 120-122	1090.71	3.6	−12.5	3.7	2.7	195	0.12	
101-2, 90-92	1091.91	8.5	−11.5	13.1	1.8	260	1.98	8
103-1, 51-53	1108.02	0.52	−27.9	1.1	1.3	260	0.09	
104-2, 124-126	1119.25	17.8	1.1	15.3	3.2	230	1.24	
104-3, 27-29	1119.78	9.2	4.7	12.1	2.1	220	0.75	9
105-1, 116-118	1126.67	13.2	12.1	16.9	2.2	220	0.70	
107-2, 11-13	1145.12	13.5	−8.5	16.0	2.3	260	1.56	10
108-1, 62-64	1153.13	13.5	−12.2	17.8	2.1	340	1.18	
109-1, 21-23	1153.72	17.7	8.0	21.5	2.3	140	1.61	
111-1, 73-75	1162.24	20.5	4.4	13.8	4.1	170	0.70	11
112-1, 63-65	1166.64	24.5	23.0	12.6	5.4	230	1.41	
113-1, 5-7	1171.06	23.0	−6.5	18.8	3.4	180	1.47	12a
113-1, 109-111	1172.10	13.5	−3.4	12.5	3.0	230	1.23	
117-1, 121-123	1190.72	10.9	−22.3	11.3	2.7	190	(0.13)	
118-1, 25-27	1194.26	11.2	−29.0	12.4	2.5	250	1.17	12b
121-1, 33-35	1207.84	6.9	−32.9	14.5	1.3	240	2.03	
123-1, 52-54	1223.03	11.0	14.6	12.4	2.5	230	1.47	
126-1, 151-153	1251.02	13.7	11.5	8.4	4.5	170	0.84	
127-1, 83-85	1254.34	9.3	8.8	8.8	2.9	180	0.97	13
128-1, 27-29	1261.28	19.2	9.0	10.6	5.0	200	1.15	
129-1, 93-95	1270.94	7.8	5.0	10.7	2.0	250	1.43	
129-2, 18-20	1271.69	9.0	−3.0	12.2	2.0	270	0.95	14
130-1, 77-79	1279.78	7.0	−7.6	9.8	2.0	250	0.89	
131-1, 129-131	1288.80	6.8	2.6	10.9	1.7	270	0.92	
132-1, 17-19	1295.18	5.0	18.5	7.6	1.8	270	0.71	
132-2, 22-24	1296.73	3.4	23.4	12.6	0.7	260	1.26	
133-1, 88-90	1304.89	31.2	14.7	14.9	5.8	240	1.74	15
133-2, 17-19	1305.68	20.3	9.4	10.6	5.3	220	(0.22)	
134-1, 47-49	1313.48	36.3	19.5	10.5	9.6	210	1.51	
136-1, 82-84	1322.83	18.5	37.3	10.2	5.0	210	0.77	
137-1, 54-56	1327.55	22.2	36.3	13.6	4.5	250	1.32	
138-1, 28-30	1332.29	18.1	−45.0	13.0	3.9	170	1.45	16

Note: *Is* = stable inclination after available AF demagnetization; magnetic unit based on stable inclination; data in parentheses are doubtful.

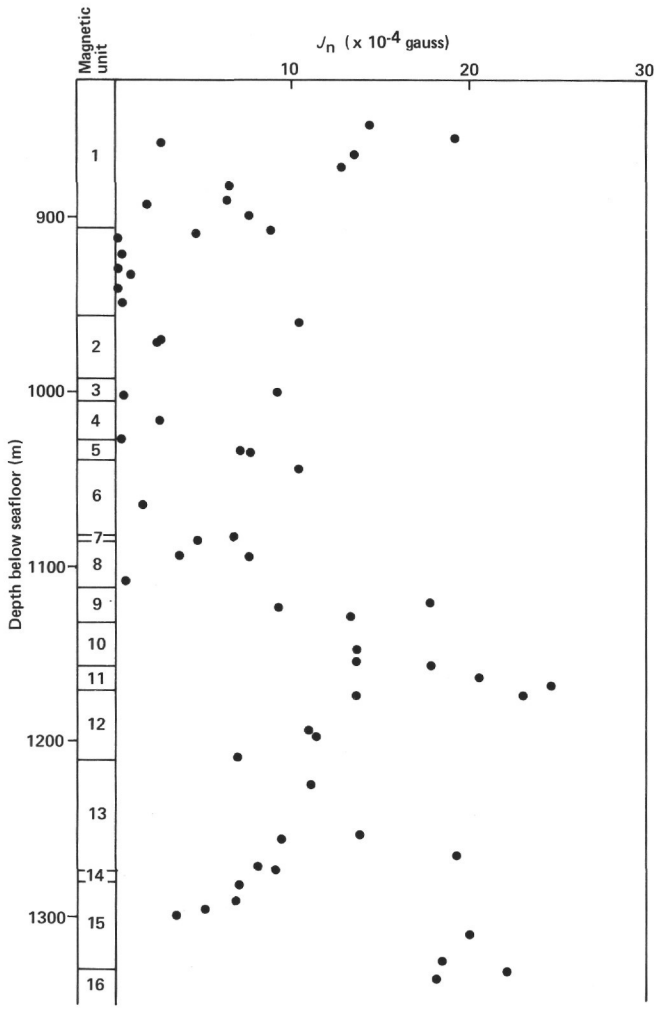

Figure 1. Intensity of NRM plotted against depth in Leg 83, Hole 504B samples. From 910 m to 1025 m the intensity of NRM is quite weak, less than 10^{-4} gauss, and this part is correlated to the high hydrothermal alteration zone.

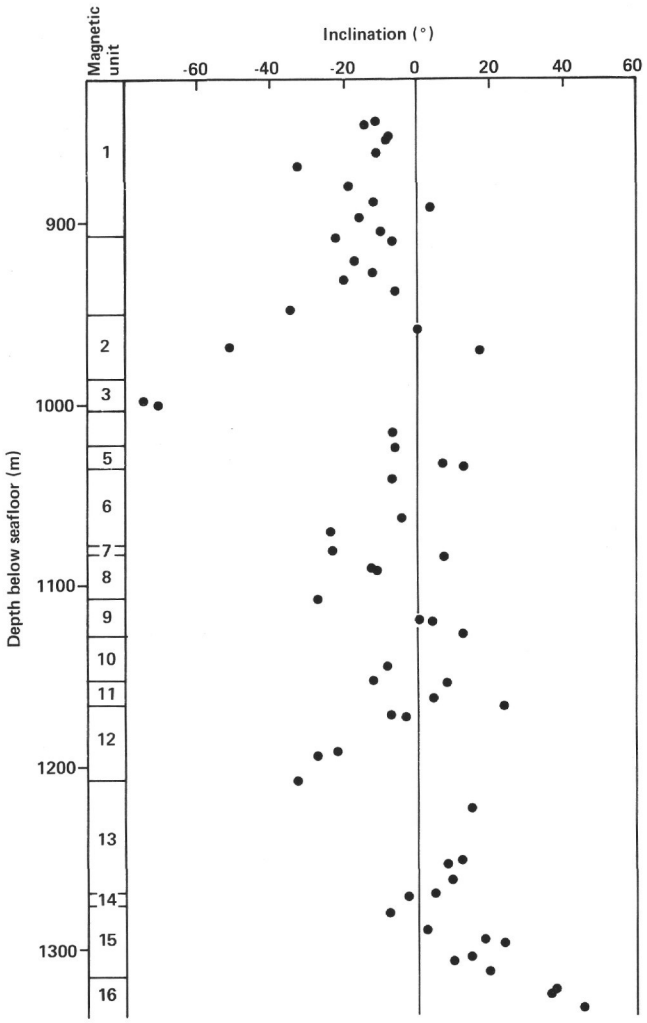

Figure 2. Stable inclinations plotted against depth in Leg 83, Hole 504B samples. The present geomagnetic inclination at Site 504C is 18.1° (downward). Magnetic units are based on the stable inclination.

Table 2. Average magnetic properties of magnetic units, Hole 504B, Leg 83.

Magnetic unit	N	J_n ($\times 10-4$ gauss)	I_s (o)	k ($\times 10-4$ gauss/Oe)	Q_n	MDF (Oe)	J_s (emu/g)
1a	11	8.9	−14	21.1	1.3	180	1.44
1b	6	0.3	−16	1.9	0.4	295	0.15
2a	1	9.3	0	9.4	2.8	250	0.8
2b	1	2.5	−52	1.5	4.6	380	0.1
2c	1	2.3	17	1.3	4.9	460	0.1
3a	2	0.4	−32	0.7	1.5	315	0.1
3b	2	4.7	−72	6.1	1.6	320	0.15
4	3	1.1	−8	2.0	1.5	330	0.13
5	2	7.4	10	12.3	1.7	250	1.46
6a	1	10.3	−6	6.4	4.5	330	0.55
6b	3	14.2	−29	4.3	7.6	300	0.4
7	1	4.6	7	2.4	6.7	240	0.12
8	3	4.2	−17	6.0	1.9	238	0.73
9	3	13.4	6	14.8	2.5	236	0.9
10	2	13.5	−10	16.9	2.2	300	1.4
11	3	21.0	12	16.0	3.9	180	1.24
12a	2	18.0	−6	15.6	3.2	205	1.35
12b	3	9.7	−28	12.7	2.2	227	1.11
13	5	12.2	10	10.2	3.4	206	1.2
14	2	8.0	−5	11.0	2.0	260	0.92
15	8	17.9	20	11.4	4.3	241	1.1
16	1	18.0	−45	13.0	3.9	170	1.45

Note: Magnetic units based on stable inclination.

lar steep inclination was also recognized in the upper part of this hole (Cores 61 through 65; Furuta and Levi, 1983). Normal magnetization zones are predominant near the bottom of the hole. These zones consist of coarse-grained doleritic rocks, characterized by high J_n.

Initial Susceptibility (k) and Koenigsberger Ratio (Q_n)

The initial susceptibility (k) is primarily controlled by the volume concentration of ferromagnetic minerals as well as by the grain size. Values of k vary from 0.9 to 34.4 $\times$ 10^{-4} gauss/Oe (Table 1) through the hole. The mean k of the hole is around 1 x 10^{-3} gauss/Oe. There is a significant decrease of k between 910 and 960 m BSF, which seems again to be related to the hydrothermal alteration.

Values of Q_n (the ratio of remanence to induced magnetization) are listed in Table 1, and generally correlate well with J_n. However, the Q_n values of all the samples are rather low, and the Q_n values of 20% of the Leg 83 samples are less than 1. The mean Q_n value is around 3. The low Q_n and relatively high k values suggest that minerals carrying initial natural remanent magnetization might be influenced by some processes.

Saturation Magnetization (J_s)

Saturation magnetization depends basically on the amounts of ferromagnetic components. Values of J_s for the minicore samples range from 0.06 to 2.6 emu/g. J_s of massive lava flows is on average larger than that of pillow lava in the hole. Microscopic observation indicates that hydrothermal alteration probably reduced the J_s, as ferromagnetic minerals (titanomagnetite) were oxidized toward titanomaghemite and/or replaced clay minerals. Maghemitization and replacement process of titanomagnetite in ordinary natural oceanic basalts are being studied in more detail by the present authors and will be presented elsewhere.

Thermal Analyses and Curie Temperatures (T_c)

Temperature dependence of the saturation magnetization was measured on all samples. A small tip of rock (100 mg) was heated at a rate of 6°C/min., kept at 650°C for 10 min., and then cooled down to room temperature at the same rate. The cycle of heating and cooling was accomplished in a vacuum of 10^{-2} Pa or less. Two types of thermomagnetic curves were recognized: reversible (Fig. 3A) and irreversible (Fig. 3B, C) ones. The latter is commonly observed in submarine pillow basalts. The Curie temperatures of these samples range from 440° to 585°C, but most of the Curie temperatures are distributed between 560° and 580°C, showing a predominance of ferromagnetic minerals of nearly pure magnetite composition. The thermomagnetic behavior of the samples shows the most ferromagnetic minerals are more or less oxidized through unmixing process of Ti-rich titanomagnetite to reproduce titanium-poor titanomagnetites (Buddington and Lindsley, 1964; O'Reilly and Banerjee, 1967; Ozima and Larson, 1970; Kinoshita and Aoki, 1972; Nishitani and Kono, 1983).

Comparison of the Leg 83 Section and the Upper Part of Hole 504B

The stable magnetic polarization of rocks from the Leg 83 section of Hole 504B carry predominantly reverse magnetization, with inclination values similar to the upper part of this hole (Furuta and Levi, 1983). However, several magnetic properties—intensity of NRM, initial susceptibility, and saturation magnetization—are different between the upper and the lower parts. In particular, J_n of the lower part is one order of magnitude

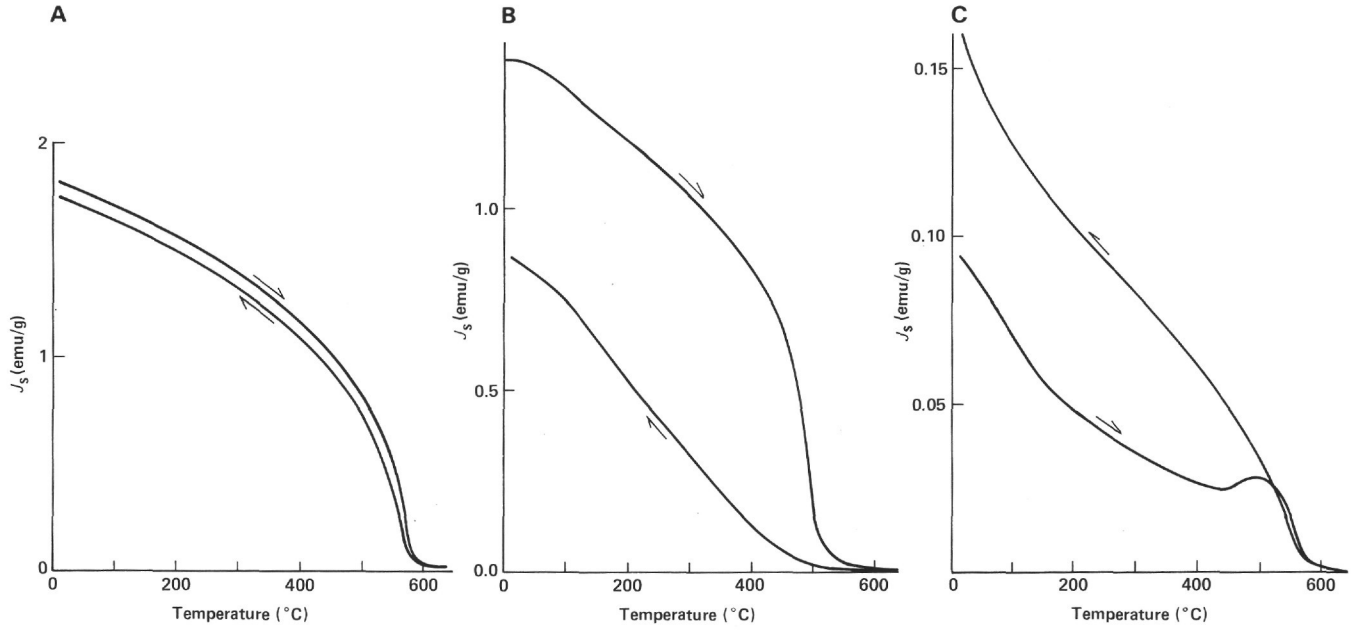

Figure 3. Typical thermomagnetic curves. A. Thermally reversible with high J_s, Sample 504B-133-1, 88–90 cm. B. Thermally irreversible with high J_s, Sample 504B-72-2, 105–107 cm. Thermally irreversible with low J_s, Sample 504B-103-1, 51–53 cm.

smaller than that of the upper part. This suggests that the alteration of magnetic minerals has been more active in the lower part. The boundary between apparently low and high alteration layers is considered from mineralogical studies to be at around 1000 m BSF (Alt et al., this volume). In particular, ferromagnetic minerals in pillow basalts are considerably influenced by hydrothermal alteration, because the grain-size of ferromagnetic minerals in pillow basalts is finer than grain size in those from massive flows. The J_n of pillow basalts from the lower part of the hole is two orders of magnitude smaller than that of the upper part. Ferromagnetic minerals in pillow samples could hardly be analyzed under the reflection microscope (most may have been replaced and changed to clay minerals). Saturation magnetization and initial susceptibility of pillow basalts are also small.

ALTERATION RELATED TO ROCK MAGNETIZATION

It is well accepted that titanomagnetite in submarine basalts undergoes more or less a maghemitization fairly shortly after the intrusion (or eruption); in some cases the time involved is much less than a few Ma. Factors or catalysts of this process have long been investigated but are not completely understood yet. Some researchers suggest that the maghemitization is a product of the low-temperature oxidation reaction of stoichiometric titanomagnetite. The process seems to be activated by applying mechanical or thermal external energies in some cases (Ozima and Sakamota, 1971; Ozima et al., 1974). However, recent experimental studies of maghemitization by means of direct, quantitative, oxygen analysis using a microfocused electron probe microanalyzer revealed that the maghemitization process is much more complicated phenomenon than it has been thought to be (Furuta, Otsuki, and Akimoto, in prep.). It is suggested that the maghemitization process starts either from stoichiometric titanomagnetite (i.e., high-temperature stable phase as noted by Buddington and Lindsley, 1964) or in a reverse manner, starting from a state somewhere between pseudobrookite and hematite (Oshima, pers. comm.; Akimoto, Kinoshita, and Furuta, in prep). In the case of naturally occurring maghemite these processes might occur simultaneously because of the possibility that stable, solid phases of titanomagnetite and hemoilmenite coexist when the basaltic magma is quenched after eruption.

The oxidation and/or reduction process seems to be highly influenced by environmental conditions controlled by external factors, such as hydrothermal alterations of mineral assemblages. Magnetization of ferromagnetic minerals is a kind of secondary physical parameter which is highly influenced by a change in physical and chemical conditions of the magnetized body. As a result of the feeble pinning mechanisms of ferromagnetic domain structures within the multidomain size of ferromagnetic crystals, the natural remanent magnetization may vary even with a scarcely identifiable change in the internal conditions of a magnetized body. The magnetization of a minicore-sized, seemingly homogeneous rock sample may change its character from spot to spot, sometimes even on a microscopic scale. Therefore, the present authors have investigated the alteration stages of the individual samples used for rock magnetic study, in order to understand the variations of rock magnetic properties of the formation with respect to depth. Our present mineralogical analyses should supplement the detailed work of Alt et al. (this volume). Here we will only briefly describe the results of analyses of mineral alteration found in the individual rock magnetic minicores.

Our techniques of analysis were as follows:

Basalt and dolerite were used for microscope observation, mineral chemistry, and bulk analyses. Constituent minerals of altered rocks and veinlets were identified under the microscope, and by means of X-ray diffraction analysis (XRD) and electron microprobe analysis (EPMA).

The basalt samples were washed in doubly distilled water for analyses of trace elements (heavy metals) by X-ray fluorescence (XRF) and Ion Coupled Plasma (ICP). Powder samples were dried at 1000°C for more than two hours before the XRF analysis. One rock powder was mixed with 5g di-lithium tetraborate anhydrous ($Li_2B_4O_7$); 200 mg of lithium bromide (LiBr) were added and the mixture was heated at about 1100°C in a platinum crucible. When the mixture had melted homogeneously, it was quenched. For ICP, 100 mg of powder sample was decomposed by 10 ml of hydrofluoric acid (HF) and 5 ml of sulfuric acid (H_2SO_4). The solution was diluted with 5 ml of condensed nitric acid (HNO_3) and bidistilled water to adjust the total volume to exactly 100 ml.

Olivine

Olivine phenocrysts remain partly fresh down to 850 m BSF but most of them are altered to secondary minerals, probably saponite. Olivine phenocrysts are altered to chlorite from 890 to 1350 m BSF, and to chlorite, serpentine, or talc from 1200 to 1350 BSF (Fig. 4).

Glass

Most of the glasses are altered to green-brown-colored minerals (probably montmorillonite) above 890 m BSF. Fresh glass, part of which is altered to montmorillonite, remains fresh down to about 880 m BSF. Glass is altered to chlorite, which is one of the typical minerals of greenschist facies, from 890 to 1350 m BSF and to actinolite from 970 to 1350 m BSF. Talc and serpentine appear from about 1150 to 1350 m BSF (Fig. 4).

Feldspars

Plagioclase is dominant in both phenocrysts and in groundmass. Plagioclase remains fresh from 274 to 890 m BSF. There are many microcracks filled with clay minerals in plagioclase phenocrysts. Hydrothermal alteration is more intensive from 890 to 1100 m BSF. Twinning is discernible in unaltered phenocrysts but hydrothermal alteration destroys it. Some relict microlites and phenocrysts remain fresh. Plagioclase remains rather fresh from 1100 to 1350 m BSF (Fig. 4).

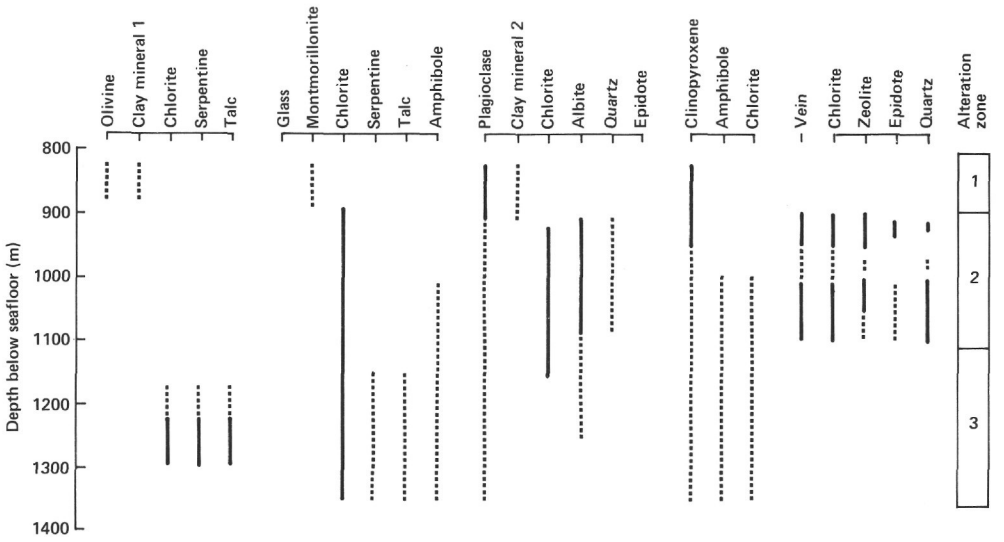

Figure 4. A schematic representation of the basaltic layer and the distribution of original minerals and secondary minerals in Leg 83 samples. Zeolite is stilbite or laumonite.

Clinopyroxene

Clinopyroxene phenocrysts are less altered than glass and other minerals. Clinopyroxene phenocrysts remain fresh from 274 to 970 m BSF but their rims are partly replaced by actinolite from 970 to 1350 m BSF (Fig. 4).

Veins

Dominant vein minerals are chlorite, laumonite, quartz, epidote, and calcite. Subordinate minerals are actinolite, pyrite, chalcopyrite, and sphalerite (Fig. 4).

Content of Heavy Metals

Trace element (heavy metal) analyses are presented in Table 3. The data are also shown graphically in Figure 5. The concentration of zinc is fairly constant, ranging from 57 to 95 ppm, both from 800 to 890 m and from 1050 to 1350 m BSF, but it is variable from 890 to 1050 m BSF, ranging from 48 to 2970 ppm.

Manganese shows the same distribution pattern with depth as zinc. Manganese content varies between 0.1 and 0.15 wt.% from 800 to 890 m and from 1050 to 1350 m BSF, but it varies between 890 and 1050 m BSF, ranging from 0.1 to 0.36 wt.%.

Cobalt content shows small variation (18–48 ppm, with an average of 39 ppm). This suggests that the upper part of the Leg 83 section of Hole 504B contains a relatively constant concentration of cobalt, and that cobalt is immobile in the reactions between basalt and hot seawater. Although nickel content varies from 8 to 141 ppm and averages 77 ppm, no systematic variation of nickle content can be observed.

Alteration Temperature Zones

The alteration temperature distribution is deduced from the sequential appearance of actinolite, chlorite, and epidote. Rocks from 274 to 890 m BSF remain fresh or are altered by low-temperature water/rock interaction, as shown by occurrence of low-temperature alteration minerals. Preliminary oxygen isotopic work suggests that these minerals formed at temperatures between 2 and 110°C (Honnorez et al., 1983), which may be the maximum temperature for basalt alteration and is probably

Table 3. Heavy metal composition, Hole 504B, Leg 83.

Core-Section (interval in cm)	Sub-bottom depth (m)	Mn (wt.%)	Zn (ppm)	Co (ppm)	Ni
71-1, 127-129	837.28	0.129	76	41	71
72-4, 38-40	848.39	0.121	71	45	48
77-2, 76-78	890.77	0.152	102	47	55
79-3, 145-147	908.96	0.167	98	39	40
80-1, 19-21	910.20	0.195	104	32	68
80-2, 27-29	911.78	0.243	1290	32	96
82-1, 21-23	928.72	0.252	115	35	131
83-1, 33-35	937.84	0.249	129	35	73
83-2, 4-6	939.05	0.195	103	39	94
84-2, 86-88	948.87	0.176	89	42	116
85-1, 57-59	956.08	0.359	2970	36	73
86-1, 13-15	964.64	0.169	102	37	45
89-1, 40-42	985.91	0.148	201	46	36
89-2, 4-7	987.06	0.186	89	43	89
90-1, 109-111	995.60	0.121	82	18	25
90-2, 101-104	997.03	0.175	87	42	141
90-3, 65-67	998.26	0.187	146	38	121
91-2, 68-70	1004.19	0.245	101	31	97
92-2, 32-34	1014.33	0.168	95	39	80
93-3, 32-34	1024.83	0.156	81	43	86
94-2, 109-111	1033.10	0.131	77	43	120
94-3, 82-84	1034.33	0.139	79	40	131
96-1, 15-17	1048.66	0.131	48	31	72
97-3, 9-11	1057.60	0.124	57	37	77
99-1, 69-71	1072.20	0.149	87	42	152
101-2, 90-92	1091.91	0.141	74	37	100
104-3, 27-29	1119.78	0.110	60	36	27
107-1, 99-101	1144.50	0.132	77	40	116
108-1, 62-64	1153.13	0.135	77	40	64
111-1, 18-24	1161.71	0.134	71	41	101
117-1, 121-123	1190.72	0.141	95	41	52
122-1, 132-134	1214.83	0.115	72	42	50
122-2, 17-19	1215.18	0.113	71	40	8
123-1, 52-54	1223.03	0.122	78	44	49
132-1, 17-19	1295.18	0.133	76	48	59
133-1, 80-82	1304.81	0.147	84	44	46
133-2, 17-19	1305.68	0.145	79	41	36

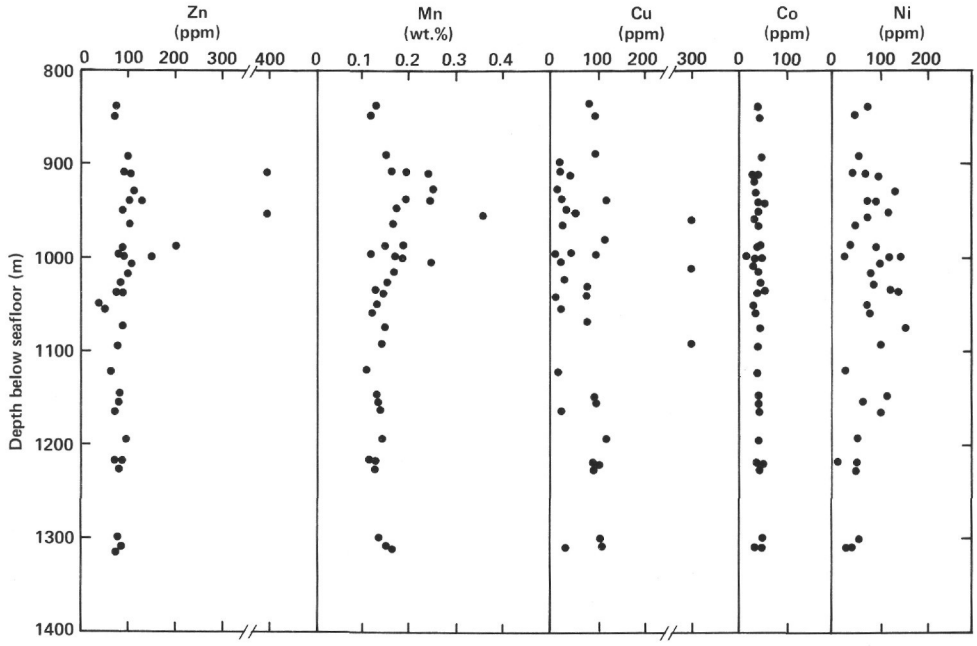

Figure 5. Downhole variation in concentrations of heavy metals in Leg 83 samples.

the maximum temperature reached above 890 m BSF (see Alt et al., this volume).

Chlorite and laumontite appear in veins below 890 m BSF. Many epidote crystals are found in the veins below 910 m BSF. Actinolite is observed below 970 m BSF. Chlorite first appears between 230° and 280°C, replacing smectite at higher temperatures, and epidote forms at temperatures as low as 200°C and becomes a major phase above 260° to 270°C in the Reykjanes geothermal system (Tomasson and Kristmannsdottir, 1972, Kristmannsdottir, 1976). The alteration temperature of actinolite-bearing assemblages is higher than 320°C in land geothermal systems (see discussion in Alt et al., this volume).

The alteration temperature deduced from these facts is shown in Figure 6. It seems that the alteration temperature increase occurred sharply between 890 and 950 m BSF.

Our data suggest that hydrothermal alteration in Hole 504B can be divided into three zones, based on the distribution of veins, appearance of secondary minerals, and content of trace elements (heavy metals).

Zone 1 (From 274 to 890 m BSF)

In Zone 1 rocks are either unaltered or altered by low-temperature (0–110°C) water-rock interaction. Metal contents show no depth dependency in this zone.

Zone 2 (From 890 to 1050 m BSF)

Alteration temperature is high. Hydrothermal solutions passed through this zone and reacted with rocks. Vein materials precipitated and some samples show high zinc and manganese contents.

Zone 3 (From 1050 to 1350 m BSF)

Alteration temperature in this zone was high. A large volume of hydrothermal solution probably did not pass

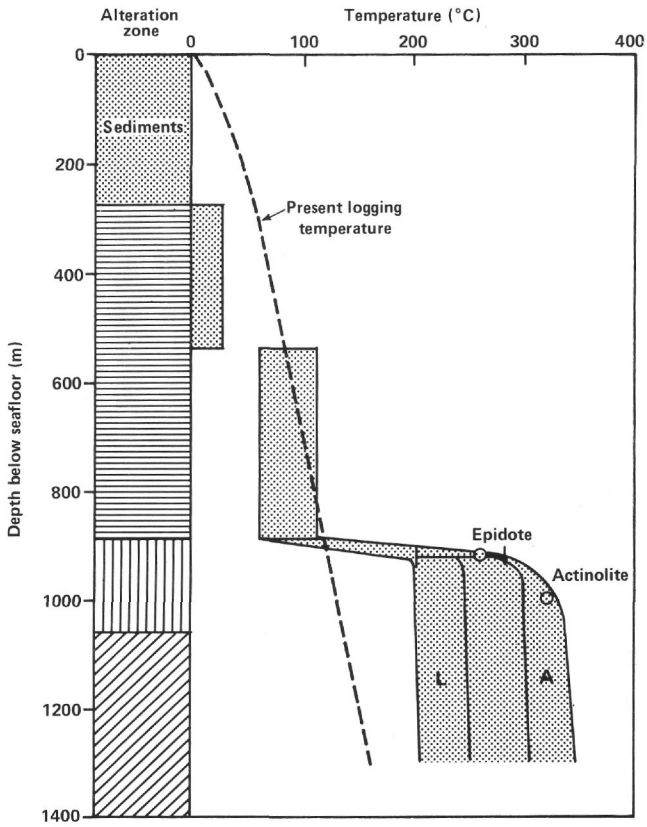

Figure 6. The alteration temperature and present logging temperature of Hole 504B as a function of depth. Alteration temperature is as follows. 274–540 m BSF: 2–30°C; 540–890 m BSF: 60–110°C; 890–1350 m BSF: 200–350°C. L = laumontite mineral assemblage (laumonite–chlorite–epidote–albite–quartz). A = actinolite mineral assemblage (actinolite–chlorite–epidote–albite–quartz).

through this zone, however, as few veins are observed in our samples. If a vast volume of hydrothermal solution had passed through the cracks, hydrothermal alteration would have been extensive along the cracks and some deposits would be observed. Metal contents show no depth dependency in this zone.

DISCUSSION AND CONCLUSIONS

Our findings about the appearance of secondary minerals are somewhat different from the results obtained by Alt et al. (this volume). Chlorite appears below 890 m BSF in our analysis and below 846 m BSF in Alt et al. (this volume). This discrepancy may be due either to different analytical methods or to the sparsity of our rock magnetic samples. Some of the montmorillonites which appear above 890 m BSF were apparently identified as chlorite if observed only under the microscope, but the chemical composition of montmorillonites and chlorite can easily be distinguished by means of EPMA.

It seems clear that the hydrothermal circulation beneath the seafloor of the Site 504 has caused a sequence of basalt alteration with greenschist facies in the deeper part of the hole. The temperature estimated from secondary minerals increases sharply between 890 and 950 m BSF. The alteration that occurred is probably due to strong hydrothermal fluid circulations.

As a result of hydrothermal circulation, magnetic minerals (titanomagnetite; $(0.5\text{–}0.7)Fe_2TiO_4 - (0.5\text{–}0.3)Fe_3O_4$; data from Furuta, 1983) first changed to titanomagnetite and then formed secondary Ti-poor titanomagnetite and pyrrhotite or pyrite. The natural remanent magnetization below 900 m BSF seems to have been remagnetized and does not reveal any dependable primary value. As a result of the hydrothermal reaction of ferromagnetic minerals, the natural remanent magnetization shows little indication of the original magnetization. More detailed analysis of the hydrothermal field and its effect on geologic formations of this area will be needed for further detailed rock magnetic discussion.

REFERENCES

Buddington, A. F., and Lindsley, D. H., 1964. Iron-titanium oxide minerals and synthetic equivalents. *J. Petrol.,* 5:310–357.

Furuta, T., 1983. Magnetic properties of basalt samples from Holes 504B and 505B on the Costa Rica Rift, Deep Sea Drilling Project Legs 69 and 70. *In* Cann, J. R., Langseth, M. G., Honnorez, J., Von Herzen, R. P., White, S. M., et al. *Init. Repts. DSDP,* 69: Washington (U.S. Govt. Printing Office), 711–720.

Furuta, T., and Levi, S., 1983. Basement paleomagnetism of Hole 504B. *In* Cann, J. R., Langseth, M. G., Honnorez, J., Von Herzen, R. P., White, S. M., et al., *Init. Repts. DSDP,* 69: Washington (U.S. Govt. Printing Office), 697–703.

Honnorez, J., Laverne, C., Hubberten, H. W., Emmermann, R., and Muehlenbachs, K., 1983. Alteration processes in Layer 2 basalts from Deep Sea Drilling Project Hole 504B, Costa Rica Rift. *In* Cann, J. R., Langseth, M. G., Honnorez, J., Von Herzen, R. P., White, S. M., et al., *Init. Repts. DSDP,* 69: Washington (U.S. Govt. Printing Office), 509–546.

Kinoshita, H. and Aoki, Y., 1972. The stability of NRM of Deccan Traps of basalts in India. *J. Geomag. Geoelectr.,* 22:459–475.

Kristmannsdottir, H., 1976. Types of clay minerals in hydrothermally altered basaltic rocks, Reykjanes, Iceland. *Jokull,* 26:30–39.

Nishitani, T., and Kono, M., 1983. Curie temperature and lattice constant of oxidized titanomagnetite. *Geophys. J. R. Astron. Soc.,* 74:585–600.

O'Reilly, W., and Banerjee, S. K., 1976. The mechanism of oxidation in titanomagnetites; a magnetic study. *Min. Mag.,* 36:29–37.

Ozima, M., Joshima, M., and Kinoshita, H., 1974. Magnetic properties of submarine basalts and the implications on the structure of the oceanic crust. *J. Geomagn. Geoelectr.,* 26:335–354.

Ozima, M., and Larson, E. E., 1970. Low- and high-temperature oxidation of titanomagnetite in relation to irreversible changes in the magnetic properties of submarine basalts. *J. Geophys. Res.,* 75: 1003–1017.

Ozima, M., and Sakamoto, N., 1971. Magnetic properties of synthesized titanomaghemite. *J. Geophys. Res.,* 67:7035–7046.

Tomasson, J., and Kristmannsdottir, H., 1972. High temperature alteration minerals and thermal brines, Reykjanes, Iceland. *Contrib. Mineral. Petrol.,* 36:123–134.

Date of Receipt: 28 September 1983
Date of Final Acceptance: 29 February 1984